

Shear-Driven Solidification of Dilute Colloidal Suspensions

Alessio Zaccone,¹ Daniele Gentili,¹ Hua Wu,¹ Massimo Morbidelli,¹ and Emanuela Del Gado²

¹*Chemistry and Applied Biosciences, ETH Zürich, CH-8093 Zürich, Switzerland*

²*Microstructure and Rheology, Institute for Building Materials, ETH Zürich, CH-8093 Zürich, Switzerland*

(Received 12 July 2010; revised manuscript received 18 December 2010; published 29 March 2011)

We show that shear-induced solidification of dilute charge-stabilized colloids is due to the interplay between shear-induced formation and breakage of large non-Brownian clusters. While their size is limited by breakage, their number density increases with shearing time. Upon flow cessation, the dense packing of clusters interconnects into a rigid state by means of grainy bonds, each involving a large number of primary colloidal bonds. The emerging picture of shear-driven solidification in dilute colloidal suspensions combines the gelation of Brownian systems with the jamming of athermal systems.

DOI: 10.1103/PhysRevLett.106.138301

PACS numbers: 82.70.Dd, 64.70.pv, 83.60.Rs

Shear-driven solidification of diluted colloidal suspensions has a dramatic impact on their applications, from industrial polymer production to natural microfluidic devices [1,2], and is a prototype of nonequilibrium transitions. If interparticle interactions are purely attractive, the applied shear stress may break down aggregates and fluidize the material [3,4]. However, the colloidal particles are often stabilized by electrostatics [1], with no tendency to aggregate at rest, and high shear rates may ultimately promote aggregation in competition with the electrostatics. The interplay between these two tendencies may lead to persistent structures [5] and this shear-induced aggregation might be as dramatic as a complete solidification of even diluted suspensions, hence seriously affecting the material and rheological properties. Although this is a widely reported phenomenon in both artificial and living systems [2,5,6], there is little understanding of the solidification mechanism. This is due to the difficulty to monitor the system with real-space optics or scattering techniques at high shear rates [5,6]. To overcome these obstacles, we have designed an experimental protocol exploiting charge-stabilized colloidal particles which interact via a typical Derjaguin-Landau-Verwey-Overbeek (DLVO) potential [1] where an energy barrier coexists with a deep, shorter-ranged attractive well. In our setup, shear-induced aggregation can be monitored in a fully controlled way, allowing us to rationalize the effect of the shear stress from an initially dilute suspension to the final solid. By combining light scattering, rheology, and microscopy data we formulate a model for the solidification mechanism. The effective packing fraction of the aggregates formed under shear increases with time. Upon flow cessation their dense packing is progressively frozen into a rigid structure by the formation of grainy (i.e., multiple) colloidal bonds which are responsible for the fairly high shear moduli observed.

Experiments.—The system consists of colloidal particles at a fixed colloid volume fraction of $\phi \approx 0.21$. For the effective DLVO interaction [1], the attractive well depth is $\approx 40k_B T$ and the repulsive barrier $\approx 60k_B T$. The colloidal

particles are surfactant-free polystyrene-acrylate latex spheres charge stabilized by the charged groups of the initiator [7]. The nearly monodisperse particles have mean radius $a \approx 60$ nm as determined from both dynamic and static light scattering (using a BI-200 SM goniometer system, Brookhaven Instruments, NY). 17 mM of NaCl were added to weakly screen the electrostatic interaction barrier, characterized by zeta-potential measurements. A strain-controlled ARES rheometer (Advanced Rheometric Expansion System, TA Instruments, Germany) with Couette geometry has been employed to induce the shear flow under shear-rate control and to measure the rheological properties. We have initially sheared the system for a varying time τ_1 at a fixed shear rate (1700 s^{-1}). For each τ_1 , upon flow cessation, we sampled the shear cell and analyzed the system by laser light scattering (LLS) using a small-angle light scattering Mastersizer 2000 instrument (Malvern, UK). The LLS analysis can be done offline since the aggregation does not evolve on the time scale of the analysis in the absence of shear. The samples were diluted at $\dot{\gamma} = 0$ to such an extent that multiple light scattering does not affect the measurement. After each τ_1 we have also performed rheological shear-sweep and frequency-sweep tests. Since the height of the energy barrier for bond breaking is $\sim 100k_B T$, the clusters are mechanically stable even under the fairly high shear rate of the Couette cell; hence, it is clear that they cannot deaggregate during offline analysis. From the scattered intensity $I(q)$ we obtain the average structure factor of the aggregates $\langle S(q) \rangle$ [8] (not to be confused with the one of the whole suspension) present in the system at the time of sampling.

Results and discussion.—The starting point of our analysis is the time evolution of the systems sheared at a constant shear rate $\dot{\gamma} = 1700 \text{ s}^{-1}$. The viscosity shows a sharp upturn in time, after an induction delay due to the activation barrier in the microscopic aggregation kinetics between two colloidal particles [9]. The barrier for shear-induced aggregation, in fact, decreases exponentially upon increasing the shear-rate and vanishes upon reaching a

certain cluster size above which the aggregation kinetics is much faster and goes with the cube of the cluster size [9]. Hence a kind of self-accelerated kinetics, leading to larger and larger aggregates, is expected once clusters of a critical size are formed. On the other hand, the action of shear is also well known to cause fragmentation, which should ultimately lead to a maximal cluster size, dictated by the mechanical balance between the stress imposed by the flow on the cluster and its mechanical response. Nevertheless, we observe (Fig. 1, main frame) that the viscosity continues to increase until the instrument stress overload threshold is reached. We have stopped the shearing after a different time duration τ_1 (*preshearing* times). For each τ_1 we have used optical microscopy and LLS to investigate the structure of the resulting suspension. An optical micrograph upon flow cessation at the largest τ_1 is shown in the inset (right) of Fig. 1. From the small-angle light scattering analysis [10], it is evident that already after a short time the size distribution of aggregates is strongly bimodal (i.e., primary particles coexist with large aggregates). The Guinier plot gives a typical aggregate radius, resulting from the competition between aggregation and breakage, $R_g \simeq 35 \pm 3 \mu\text{m}$ which remains constant with time [10], indicating that the aggregation under shear rapidly leads to an optimal cluster size. From the power-law regime of the scattering curves we extract the fractal dimension d_f of the large clusters: as a function of τ_1 [10] d_f also rapidly reaches a plateau at $\simeq 2.7 \pm 0.1$, a fairly high value which is typical of shear-driven aggregation [11] where breakage events and restructuring induced by flow stresses combine [12]. We have measured the fraction $\chi(t)$ of primary colloidal particles converted to clusters and found that it steeply increases [10]. The emerging picture is that under shear the system is constantly generating new clusters with

approximately the same size R_g and fractal dimension d_f . The fast increase in the number density of clusters which are fractal and porous is associated with a rapid increase of their effective packing fraction: this could be the reason for the sharp nonlinear increase of the viscosity in Fig. 1. To test this hypothesis, we have estimated the clusters effective packing fraction ϕ_{eff} through the relation $\phi_{\text{eff}}(t) = \chi(t)\phi k^{-1}(R_g/a)^{3-d_f}$, where k is a geometric prefactor close to 1 and ϕ is the initial volume fraction of primary particles [13]. In the inset (left) of Fig. 1 we plot the viscosity $\eta(t)$ (circles), normalized by η_0 , as a function of $\phi_{\text{eff}}(t)$. We have also calculated the high-shear viscosity of an equivalent suspension of hard spheres of the same linear size at the same volume fraction $\phi_{\text{eff}}(t)$, using the Einstein formula properly extended to high $\phi_{\text{eff}}(t)$ [14] which gives $\eta \simeq \eta_0 \exp(5\phi_{\text{eff}}(t)/2)$ (the full line in the same inset). The agreement indicates that the increase of the viscosity under shear in Fig. 1 can be ascribed indeed to the increasing packing fraction of the clusters, which hydrodynamically behave as hard spheres due to the fairly high d_f [15]: the initial dilute colloidal suspension has changed, under shear, into a suspension of non-Brownian aggregates whose packing fraction increases with the shearing time.

After each of the preshearing times, we also perform a shear-sweep experiment where $\dot{\gamma}$ is varied but kept below $\dot{\gamma} = 1700 \text{ s}^{-1}$. This guarantees that the aggregates formed during the preshearing are mechanically stable and do not break up during the shear sweep [16,17]. The data are plotted in Fig. 2. The curves correspond to $\tau_1 = 4054, 7420, 7500, 7520, \text{ and } 7555 \text{ s}$ from bottom to top, and to $\phi_{\text{eff}}(\tau_1)$ increasing accordingly. For the shortest τ_1 , a modest shear thinning is followed by a Newtonian plateau. Upon increasing τ_1 , the viscosity curves are shifted to higher values and a steep shear thickening appears: the

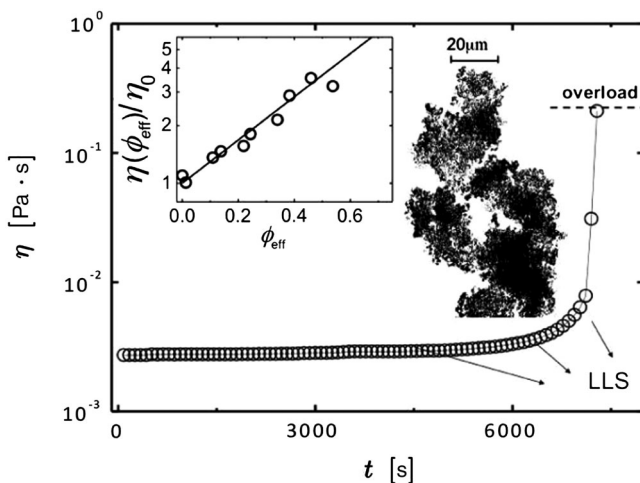


FIG. 1. Main frame: Time evolution of the viscosity η at $\dot{\gamma} = 1700 \text{ s}^{-1}$ at $\phi \simeq 0.21$. Insets: left— η/η_0 as a function of ϕ_{eff} from experiments (circles) and the extended Einstein formula (line); right—optical micrograph upon flow cessation.

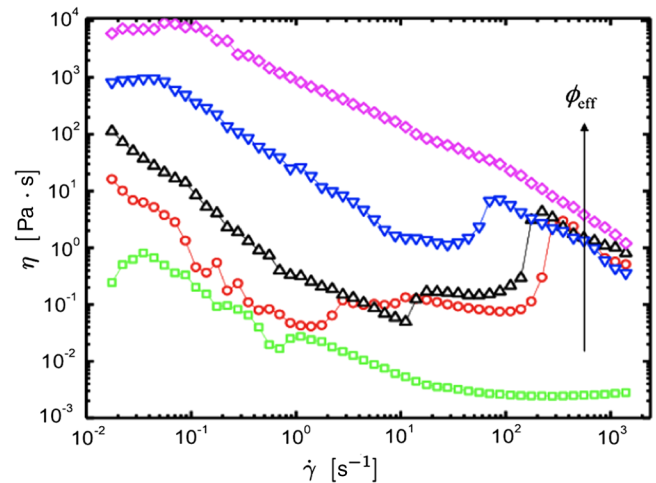


FIG. 2 (color online). Shear-sweep curves obtained after preshearing at $\dot{\gamma} = 1700 \text{ s}^{-1}$ for $\tau_1 = 4054, 7420, 7500, 7520, \text{ and } 7555 \text{ s}$ (from bottom to top).

rheological behavior of our system upon increasing τ_1 is qualitatively the same as the one of dense non-Brownian suspensions upon increasing volume fraction [18,19]. Note that flow inhomogeneity may occur in these types of measurements [20,21] and we cannot exclude its presence here (although magnetic-resonance imaging studies in a very similar system [22] detected shear banding only for $\dot{\gamma} < 60 \text{ s}^{-1}$). Thus Fig. 2 gives only macroscopic rheological information, possibly dependent on the geometry. A shear thinning followed by a shear thickening regime has also been observed in some gelling colloidal suspensions [23], where it has been explained in terms of an increase of the clusters number density due to breakup. Here we have made sure that the shear sweep is done at $\dot{\gamma}$ lower than the value needed for breaking up the clusters; therefore, we rather associate the shear thickening to the formation of interclusters bonds, possibly also promoted by hydrodynamic interactions [24] and/or from a residual intercluster attraction: the shear rate is too low to break the preformed aggregates but can promote, instead, the formation of further bonds among them. At the largest ϕ_{eff} (i.e., τ_1) the shear thickening is no longer visible. The behavior of the stress intensity σ as a function of $\dot{\gamma}$ plotted in Fig. 3 sheds some light on this rheological behavior. For large ϕ_{eff} the curves can be well described with an extended Herschel-Bulkley type of behavior, which accounts for shear thickening [25], $\sigma(\dot{\gamma}) = \sigma_y + a_1 \dot{\gamma}^{1/2} + a_2 \dot{\gamma}^{1/\epsilon}$ where σ_y is the yield stress, a_1 and a_2 are parameters depending on ϕ_{eff} , and $\epsilon < 0.1$ is typically obtained for the steep shear thickening of densely packed non-Brownian suspensions [25]. This indicates that the onset of the yield stress occurs in the range of effective volume fractions $0.50 < \phi_{\text{eff}} < 0.56$. At $\phi_{\text{eff}} \approx 0.66$, i.e., the largest value obtained here, the yield stress has now a value

close to the upper stress limit of the shear thickening and this makes the shear thickening no longer visible. The same phenomenon has been observed indeed in densely packed non-Brownian suspensions [18]. Hence, in a dilute colloidal system at a solid fraction $\phi = 0.21$ we get the whole rich phenomenology observed in non-Brownian suspensions upon varying the solid fraction in a broad range.

The emergence of a yield stress at sufficiently high ϕ_{eff} raises the question of how a fully solid state may form. Upon flow cessation after each preshearing time τ_1 , we have also performed dynamic frequency sweeps. The results are reported in Fig. 4. At the lowest τ_1 considered (which is, however, close to the point where the high-shear viscosity starts to rise dramatically) the system still behaves liquidlike as the loss modulus G'' is always slightly larger than the elastic modulus G' . Upon increasing τ_1 and hence ϕ_{eff} , G' takes over with respect to G'' and the ratio G'/G'' becomes larger with τ_1 , while remaining mostly constant with the frequency. This is a behavior typically observed in colloidal gels [14,26,27] and suggests that, for the longest τ_1 , upon flow cessation the clusters are not only densely packed but can also connect into a spanning, stress-bearing structure [28]. During the shearing, in fact, the aggregates are maintained in a fluid state by the imposed high shear rate, whereas upon cessation of flow the system is subjected to a rapidly decreasing stress until a quiescent state is reached. Hence interaggregates connections can gradually form and become permanent as the zero stress is reached: provided that ϕ_{eff} is high enough, a cohesive solid random packing of aggregates will form. To test this picture, we have calculated the elastic modulus of this disordered solid using the approach derived in [28], giving a quantitative estimate of the contribution to

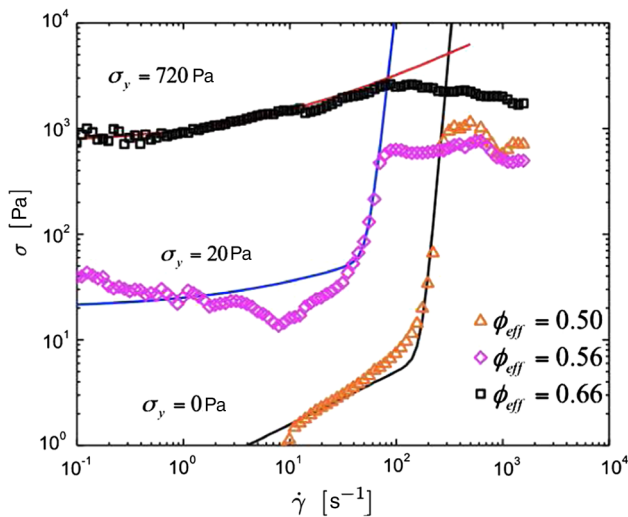


FIG. 3 (color online). The measured stress as a function of shear-rate (symbols) and the extended Herschel-Bulkley curves (lines) [25].

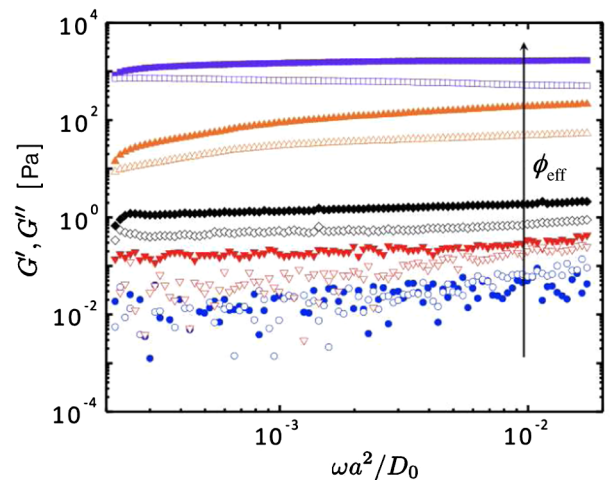


FIG. 4 (color online). G' (filled symbols) and G'' (open symbols) measured after $\tau_1 = 4054, 6350, 7400,$ and 7480 s (from bottom to top) as a function of the frequency ω in units of the diffusion time in the dilute limit, $\tau_0 = a^2/D_0$.

elasticity of interaggregate connections for an amorphous close-packed assembly of aggregates of cohesive particles:

$$G' = (2/5\pi)\tilde{\kappa}\phi_{\text{eff}}\tilde{z}R_g^{-1} \quad (1)$$

where \tilde{z} is the aggregate average coordination number, R_g is their linear size, and $\tilde{\kappa}$ is the stiffness of the interaggregate connections formed upon flow cessation. We use this result to estimate the elastic modulus of our aggregate gel formed upon flow cessation at $\phi_{\text{eff}} = 0.66$, corresponding to the largest effective cluster packing fraction and the most rigid state observed, where the affine assumption underlying Eq. (1) is reasonably applicable. The irregular aggregates morphology, visible also by optical microscopy (inset of Fig. 1), indicates that each connection is actually composed of many colloidal bonds (grainy contacts). In order to estimate the number of such bonds, we consider that for a fractal aggregate of radius R_g and fractal dimension d_f , the total number of particles is $N_c = (R_g/a)^{d_f}$, a being the particle radius. Hence $a(dN_c/dR_g) = d_f/aN_c^{(d_f-1)/d_f}$ gives the number of particles added to the outermost layer of an aggregate of radius R_g . Using $a \approx 60$ nm, $R_g \approx 35 \pm 3$ μm , and $d_f \approx 2.7$ for our system, we get the number of particles on the surface of the aggregates $\approx 136 \times 10^3$. With an average number of 7 grainy contacts per aggregate, as for densely packed spheroidal objects [29], we can estimate that each of them involves $n \approx 19.4 \times 10^3$ particles, consistent with the value $n \approx 21 \times 10^3$ obtained measuring the contact area from optical micrographs. On this basis, we estimate $\tilde{\kappa} = n\kappa$, where $\kappa = (\partial^2 U_{\text{DLVO}}/\partial r^2)_{r=r_{\text{min}}} \approx 2 \times 10^{-5}$ N/m. Hence, we finally obtain for the elastic modulus of our dense gel formed upon flow cessation, $G' \approx 760$ Pa, consistent with the value measured experimentally $G' \approx 843$ Pa at the largest ϕ_{eff} (see Fig. 4).

Conclusions.—Our experiments rationalize the shear-induced solidification of a dilute, stable colloidal suspension in a fully controlled way. Large aggregates of a typical size are continuously generated under shear and behave hydrodynamically like non-Brownian hard spheroids. Varying the shearing time leads to the same rheological response of dense non-Brownian suspensions upon varying the solid fraction. Upon flow cessation, these aggregates can eventually form cohesive random packings where each interaggregate bond involves a large number of colloidal bonds. Such a solidification mechanism is thus a hybrid between colloidal gelation [30] and the packing-driven jamming [31] of non-Brownian suspensions (pastes, slurries). This scenario gives a novel insight into the complexity of the shear-induced solidification of colloidal dispersions of practical relevance.

This work was supported by SNSF (Grant No. 200020-126487/1). E. D. G. is supported by the SNSF (Grant No. PP002_126483/1).

- [1] W. B. Russel, D. Saville, and W. R. Schowalter, *Colloidal Dispersions* (Cambridge University Press, Cambridge, 2001).
- [2] N. A. Mody and M. R. King, *Biophys. J.* **95**, 2539 (2008); S. Rammensee *et al.*, *Proc. Natl. Acad. Sci. U.S.A.* **105**, 6590 (2008); K. M. N. Oates *et al.*, *J. R. Soc. Interface* **3**, 167 (2006).
- [3] J. Vermant and M. J. Solomon, *J. Phys. Condens. Matter* **17**, R187 (2005).
- [4] A. J. Liu and S. R. Nagel, *Nature (London)* **396**, 21 (1998).
- [5] D. Xie *et al.*, *Soft Matter* **6**, 2692 (2010).
- [6] M. Vasudevan *et al.*, *Nature Mater.* **9**, 436 (2010); I. Wunderlich, H. Hoffmann, and H. Rehage, *Rheol. Acta* **26**, 532 (1987).
- [7] A. Zaccone *et al.*, *J. Phys. Chem. B* **112**, 1976 (2008).
- [8] P. Dimon *et al.*, *Phys. Rev. Lett.* **57**, 595 (1986).
- [9] A. Zaccone *et al.*, *Phys. Rev. E* **80**, 051404 (2009).
- [10] See supplemental material at <http://link.aps.org/supplemental/10.1103/PhysRevLett.106.138301> for laser light scattering analysis.
- [11] P. B. Warren, R. C. Ball, and A. Boelle, *Europhys. Lett.* **29**, 339 (1995).
- [12] V. Becker *et al.*, *J. Colloid Interface Sci.* **339**, 362 (2009); M. L. Eggersdorfer *et al.*, *J. Colloid Interface Sci.* **342**, 261 (2010).
- [13] A. Zaccone, Ph.D. thesis, ETH Zurich, 2010.
- [14] R. G. Larson, *The Structure and Rheology of Complex Fluids* (Oxford University Press, New York, 1999), p. 266.
- [15] P. G. de Gennes, *Scaling Concepts in Polymer Physics* (Cornell Univ. Press, Ithaca, NY, 1979), p. 176.
- [16] A. Zaccone *et al.*, *Phys. Rev. E* **79**, 061401 (2009).
- [17] A. S. Moussa *et al.*, *Langmuir* **23**, 1664 (2007).
- [18] E. Brown and H. M. Jaeger, *Phys. Rev. Lett.* **103**, 086001 (2009).
- [19] E. Bertrand, J. Bibette, and V. Schmitt, *Phys. Rev. E* **66**, 060401 (2002).
- [20] A. Fall *et al.*, *Phys. Rev. Lett.* **105**, 268303 (2010); A. Fall, J. Paredes, and D. Bonn, *Phys. Rev. Lett.* **105**, 225502 (2010).
- [21] C. Bonnoit *et al.*, *Phys. Rev. Lett.* **105**, 108302 (2010); C. Bonnoit *et al.*, *J. Rheol.* **54**, 65 (2010).
- [22] P. C. F. Moller *et al.*, *Phys. Rev. E* **77**, 041507 (2008).
- [23] C. O. Osuji, C. Kim, and D. A. Weitz, *Phys. Rev. E* **77**, 060402 (2008).
- [24] B. J. Maranzano and N. J. Wagner, *J. Chem. Phys.* **117**, 10 291 (2002).
- [25] E. Brown *et al.*, *Nature Mater.* **9**, 220 (2010).
- [26] V. Trappe and D. A. Weitz, *Phys. Rev. Lett.* **85**, 449 (2000).
- [27] M. R. Mackley *et al.*, *Chem. Eng. Sci.* **49**, 2551 (1994).
- [28] A. Zaccone, H. Wu, and E. Del Gado, *Phys. Rev. Lett.* **103**, 208301 (2009).
- [29] P. M. Chaikin *et al.*, *Ind. Eng. Chem. Res.* **45**, 6960 (2006).
- [30] E. Del Gado *et al.*, *Europhys. Lett.* **63**, 1 (2003); A. Fierro *et al.*, *J. Stat. Mech.* (2008) L04002; E. Del Gado and W. Kob, *Soft Matter* **6**, 1547 (2010); P. N. Segre *et al.*, *Phys. Rev. Lett.* **86**, 6042 (2001).
- [31] M. E. Cates *et al.*, *Phys. Rev. Lett.* **81**, 1841 (1998).